

## Oncolytic measles virus efficacy in murine xenograft models of atypical teratoid rhabdoid tumors

Adam W. Studebaker, Brian Hutzen, Christopher R. Pierson, Terri A. Shaffer, Corey Raffel, and Eric M. Jackson

Center for Childhood Cancer and Blood Diseases, Research Institute at Nationwide Children's Hospital, Columbus, Ohio (A.W.S., B.H.); Nationwide Children's Hospital Department of Pathology and Laboratory Medicine and Departments of Pathology and Anatomy, The Ohio State University College of Medicine, Columbus, Ohio (C.R.P.); Animal Resources Core, Research Institute at Nationwide Children's Hospital, Columbus, Ohio (T.A.S.); Department of Neurological Surgery and Pediatrics, University of California, San Francisco, California (C.R.); Department of Neurosurgery, Johns Hopkins University, Baltimore, Maryland (E.M.J.)

**Corresponding Author:** Adam W. Studebaker, PhD, Center for Childhood Cancer and Blood Diseases, Nationwide Children's Hospital, Columbus, OH 43205 (adam.studebaker@nationwidechildrens.org).

**Background.** Atypical teratoid rhabdoid tumor (AT/RT) is a rare, highly malignant pediatric tumor of the central nervous system that is usually refractory to available treatments. The aggressive growth, propensity to disseminate along the neuroaxis, and young age at diagnosis contribute to the poor prognosis. Previous studies have demonstrated the efficacy of using oncolytic measles virus (MV) against localized and disseminated models of medulloblastoma. The purpose of this study was to evaluate the oncolytic potential of MV in experimental models of AT/RT.

**Methods.** Following confirmation of susceptibility to MV infection and killing of AT/RT cells in vitro, nude mice were injected with BT-12 and BT-16 AT/RT cells stereotactically into the caudate nucleus (primary tumor model) or lateral ventricle (disseminated tumor model). Recombinant MV was administered either intratumorally or intravenously. Survival was determined for treated and control animals. Necropsy was performed on animals showing signs of progressive disease.

**Results.** All cell lines exhibited significant killing when infected with MV, all formed syncytia with infection, and all generated infectious virus after infection. Orthotopic xenografts displayed cells with rhabdoid-like cellular morphology, were negative for INI1 expression, and showed dissemination within the intracranial and spinal subarachnoid spaces. Intratumoral injection of live MV significantly prolonged the survival of animals with intracranial and metastatic tumors.

**Conclusion.** These data demonstrate that AT/RT is susceptible to MV killing and suggest that the virus may have a role in treating this tumor in the clinical setting.

**Keywords:** atypical teratoid rhabdoid tumor, intravenous, measles virus, oncolytic virus.

Atypical teratoid/rhabdoid tumors (AT/RTs) are highly aggressive brain tumors that predominantly afflict young children. AT/RTs are usually composed of rhabdoid cells intermingled with varying amounts of neuroepithelial, mesenchymal, and epithelial elements and are frequently associated with genetic alterations of *SMARCB1* (*INI1/hSNF5*), a tumor-suppressor gene located on chromosome 22.<sup>1–6</sup> Traditional therapies used to treat other pediatric brain tumors (ie, surgical resection, chemotherapy, and radiation) are associated with significant neurocognitive morbidity and are not effective in producing long-term survival in patients with AT/RT. Contributing to the poor prognosis is the young age (<3 years) of the majority of patients with these tumors, which limits the extent of

treatment, particularly radiation. Currently, the survival rate of children younger than aged 3 years is <15%; thus, there is a great need for the development of alternative strategies in the treatment of AT/RT.<sup>7</sup>

Oncolytic viruses are rapidly emerging as potentially useful anticancer drugs.<sup>8</sup> An oncolytic virus is one that selectively propagates and destroys cancerous tissue without causing excessive damage to the normal surrounding tissue.<sup>9</sup> Oncolytic measles virus (MV) is one such virus that has demonstrated promising results in preclinical testing<sup>10–13</sup> and clinical trials.<sup>14–16</sup> The MV used in antitumor studies is a derivative of the Edmonston vaccine strain. This virus has a remarkable track record that spans more than 50 years and over a billion

Received 31 December 2014; accepted 11 March 2015

© The Author(s) 2015. Published by Oxford University Press on behalf of the Society for Neuro-Oncology. All rights reserved.

For permissions, please e-mail: journals.permissions@oup.com.

human recipients worldwide. The reversion of the vaccine strain back to pathogenic MV has never been documented. The vaccine strain displays a natural tropism for the CD46 membrane protein, an inhibitory complement regulator strongly overexpressed by many types of tumor relative to normal tissue.<sup>17,18</sup> MV preferentially infects tumor cells and induces their death via syncytia formation and apoptosis, causing minimal damage to the normal surrounding tissue.<sup>19,20</sup> In recently published studies, we demonstrated that MV virotherapy was effective against orthotopic mouse xenograft models of localized and disseminated medulloblastoma, the most common malignant brain tumor in children.<sup>21,22</sup>

In this study, we have investigated the ability of a modified Edmonston strain of MV to kill AT/RT cells in vitro and in vivo. In vitro killing of AT/RT cells from established cell lines was investigated at various multiplicities of infection (MOIs). Using established orthotopic models of AT/RT, in which cells are injected into the brain (localized model) or lateral ventricle (disseminated model) of immunocompromised mice, the efficacy of MV in prolonging life in the injected animals was determined. Here, we show that MV is an effective therapeutic agent against in vitro and in vivo models of AT/RT. Overall, the results reported here suggest that use of modified MV may represent an effective new treatment for AT/RT.

## Materials and Methods

### Cell Culture

The Vero (African green monkey) cell line was obtained from the American Type Culture Collection. Human AT/RT cell lines BT-12 and BT-16 were supplied by Dr. Peter J. Houghton (Nationwide Children's Hospital, Columbus, Ohio) and have been described previously.<sup>23</sup> Vero and AT/RT cells were grown in Dulbecco's modified Eagle's medium (DMEM) supplemented with 10% or 20% fetal bovine serum (FBS), respectively, at 37°C in a humidified incubator set at 5% CO<sub>2</sub>. The BT-12- and BT-16-luciferase cell lines were generated using a method previously described.<sup>21</sup> Luciferase bioluminescence emitted per cell line was quantified. BT-12-luciferase and BT-16-luciferase cells ( $5 \times 10^4$ ) were plated in replicates of 6 in a well of a white 96-well plate. Twenty-four hours later, Bright-Glo reagent (Promega) was added to each well. A Victor2 Wallac plate reader (Perkin Elmer) was used to measure light emissions in counts per second (CPS) over a 10-second period. Data were quantified as CPS/cells.

### Production of Measles Virus

The MV-green fluorescent protein (GFP) virus was rescued, as previously described, and propagated in Vero cells at a MOI of 0.01 for 2 hours at 37°C.<sup>21</sup> Following incubation, the medium containing unabsorbed virus was replaced with DMEM supplemented with 10% FBS. Cells were incubated for 48 hours at 37°C and then transferred to 32°C for 24 hours. The presence of EGFP-positive cells was verified by fluorescence microscopy. Medium was gently aspirated, and cells were collected in Opti-MEM (Invitrogen). Virus was harvested by 2 cycles of freezing and thawing. The titer of the virus was determined by 50% tissue culture infective dose (TCID<sub>50</sub>) titration on Vero cells.<sup>24</sup>

### Assessment of Cytopathic Effect in Vitro

Cells were plated in 6-well plates at a density of  $1 \times 10^5$  cells per well. Twenty-four hours after seeding, the cells were infected with MV-GFP in triplicate at different MOIs of 0.1 and 1 in 1 ml of Opti-MEM for 2 hours at 37°C. Each MOI was performed in triplicate wells. At the end of the incubation period, the virus was removed, and the cells were maintained in DMEM containing 10% FBS. The same number of uninfected cells in 6-well plates was used as controls. Cells were monitored under a microscope for the appearance of syncytia over the next 72 hours and photographed with a Spot RT KE/SE digital camera (Diagnostic Instruments Inc.). The number of viable cells in each well was counted using a hemocytometer at 2, 3, and 4 days after infection. Viable cells were identified using trypan blue exclusion. The percentage of surviving cells was calculated by dividing the number of viable cells in the infected well by the number of viable cells in the uninfected well corresponding to the same time point. Infection was confirmed using fluorescent microscopy at the corresponding time points.

### In Vitro Virus Production Assays

BT-12 ( $5 \times 10^5$  cells/well) and BT-16 cells ( $1 \times 10^6$  cells/well) were seeded in 6-well plates and infected the following day with MOIs of 0.1 and 0.5 MV in 500  $\mu$ L OptiMEM. Unabsorbed virus was removed after 2 hours and replaced with 3 ml fresh DMEM. The cells were scraped into 125  $\mu$ L Opti-MEM at 24, 48, or 72 hours after infection, freeze-thawed twice, and centrifuged. The titer of collected MV was then measured on Vero cells using the TCID<sub>50</sub> method. Samples were assayed in triplicate.

### In Vivo Xenograft Studies

Localized and disseminated models were utilized as described previously.<sup>21,22</sup> In brief,  $5 \times 10^5$  BT-12 or BT-16 cells suspended in 2  $\mu$ L PBS were implanted into the caudate nucleus (localized model) or right lateral ventricle (disseminated model) of 5-week-old Hsd:ATHymic Nude-Foxn1nu mice (Harlan Laboratories). Bioluminescent imaging was conducted prior to initiating treatment to ensure that tumor burdens were roughly equivalent. Animals exhibiting a positive bioluminescent signal in their spinal cords were classified as having disseminated disease (see Supplementary Fig. S1).<sup>22</sup> Treatment with MV-GFP ( $5 \times 10^5$  pfu/dose) or an equivalent dose of UV-inactivated MV-GFP was injected intratumorally 7 days after tumor implantation for the localized AT/RT mice or 3 days for the disseminated model mice. MV-GFP ( $1 \times 10^6$  pfu/dose) or an equivalent dose of UV-inactivated MV-GFP was injected intravenously via the lateral tail vein at 7, 9, and 11 days after tumor implantation.

The animals were euthanized if they developed neurological deficits such as hemiparesis or lethargy. At the time of necropsy, brains were collected, fixed overnight with 10% formalin, paraffin embedded, cut into 5  $\mu$ m tissue sections, and stained with hematoxylin and eosin (H&E). All animal experiments were approved by the Nationwide Children's Hospital Institutional Animal Care and Use Committee.

### ***In Vivo Bioluminescence Imaging***

Bioluminescence imaging studies were conducted prior to each MV-GFP injection, then weekly thereafter using the Xenogen Ivis Spectrum (Caliper Life Sciences). Animals received an intraperitoneal injection of 4.5  $\mu$ g XenoLight RediJect D-Luciferin (Caliper Life Sciences) and were continuously maintained under isoflurane gas anesthesia. Images were obtained 20 minutes after luciferin administration. The bioluminescence intensity was quantified using Living Image Software (version 3.1, Caliper). Signal intensity was quantified as the sum of detected photons per second within the region of interest. The lower threshold of detection was set at 1250 photons/sec/cm<sup>2</sup>/sr.

### ***Histopathological Evaluation***

At the time of necropsy, brains and decalcified spinal columns were fixed overnight in 10% buffered formalin phosphate. They were then paraffin embedded, cut into 4  $\mu$ m tissue sections, and stained with H&E. Individual sections were visualized under a Zeiss Axioskop 2 Plus microscope and photographed with a Zeiss AxioCam MRC camera (Carl Zeiss MicroImaging).

### ***Immunohistochemistry***

Immunohistochemistry (IHC) was performed on paraffin-embedded tissues. IHC of tissue slides with anti-Measles nucleoprotein antibody (NB100-1856, Novus Biologicals) was carried out as described previously.<sup>22</sup> Immunostaining for anti-INI-1 antibody was performed using a Bond-max automated immunostainer (Leica Microsystems). Sections underwent heat-induced antigen retrieval in Novocastra Bond Epitope Retrieval Solution 2 (Leica Biosystems) for 20 minutes. Purified mouse anti-INI-1 clone MRQ-27 (prediluted, Cell Marque) was applied at room temperature for 15 minutes and washed. Visualization was performed using Novocastra Bond Polymer Refine Red Detection (Leica Biosystems) with diaminobenzidine (Leica Biosystems) as the final chromagen. INI-1 immunoreactivity of neoplastic nuclei was compared with surrounding nonneoplastic cell nuclei within the same microscopic field. INI-1 immunoreactivity was absent in tumor nuclei, while adjacent nonneoplastic nuclei were immunoreactive. The sections were reviewed by the neuropathologist author (C.R.P.).

### ***Statistical Analysis***

Survival curves were generated using the Kaplan-Meier method and GraphPad Prism 5 software. Statistical significance ( $P < .05$ ) between the groups was determined using the log-rank test. All other statistical analysis was performed using Microsoft Office Excel (v.11.6560.6568 SP2) in data analysis using regression or Student's *t* test (paired 2 sample for means). Probabilities for the Student's *t* test are listed as " $P(T \leq t)$  2-tail" with an alpha of 0.05.

## **Results**

### ***Measles Virus Replicates and Causes Significant Cytopathic Effect in Atypical Teratoid Rhabdoid Tumor Cell Lines in Vitro***

Two AT/RT cell lines (BT-12 and BT-16) were examined for their susceptibility to MV infection and killing in vitro. A MV containing

the GFP gene as a marker for infection (MV-GFP) was used. Both cell lines exhibited significant infection with MV-GFP, each displaying the presence of green fluorescent syncytia (BT-12, Fig. 1A; BT-16, Fig. 1B). To evaluate whether MV could infect stem cells derived from AT/RT cells, cells were grown and maintained as neurospheres.<sup>25</sup> BT-12 (Fig. 1C) and BT-16 (Fig. 1D) were susceptible to MV infection when propagated as neurospheres.

The viability of BT-12 (Fig. 2A) and BT-16 (Fig. 2B) human AT/RT cells following administration of MV-GFP was evaluated. More than 20% of the cells were viable at 48 hours after infection at an MOI of 0.1, and <1% of the cells were viable at 48 hours after infection at an MOI of 1. By 72 hours after infection <5% of the cells were viable at an MOI of 0.1.

To determine whether MV-GFP could replicate in AT/RT cells, titers of the virus produced from these cells were measured daily after infection. As shown in Fig. 2, BT-12 (Fig. 2C) and BT-16 (Fig. 2D) supported replication of MV-GFP. Virus titers peaked 72 hours post infection in both cells when MOIs of 0.01 and 0.05 were used. Virus titers produced from cells infected at an MOI of 0.05 were higher than from cells infected at an MOI of 0.01 at 24 and 48 hours post infection, but virus titers were comparable at 72 hours post infection.

### ***Measles Virus Increases Survival of Animals with Localized Atypical Teratoid Rhabdoid Tumor Disease***

To determine the efficacy of MV-GFP in vivo, we established orthotopic xenograft models of primary and disseminated AT/RT disease. The lack of positive INI1 immunostaining in the xenograft tumors of BT-12 (Fig. 4C) and BT-16 (Fig. 4I) confirmed translation of the cells in culture to an animal model. Staining of mouse cells in the brain served as an internal positive control. To model primary disease, BT-12 (Fig. 3A) and BT-16 (Fig. 3C) cells were stereotactically injected into the right caudate putamen to establish tumors. Seven days following tumor injection, MV-GFP or UV-inactivated MV-GFP ( $5 \times 10^5$  pfu) was injected intratumorally. Animals were monitored to assess survival. There was a statistically significant prolongation of survival in MV-GFP-treated mice compared with UV-inactivated virus-treated controls ( $P > .001$ , BT-12 [Fig. 3A];  $P > .001$ , BT-16 [Fig. 3C]). The median survival for MV-GFP-treated BT-12 animals was 64 days ( $n = 9$ ; range: 31–100 days) compared with 24 days ( $n = 8$ ; range: 21–37 days) for UV-inactivated MV-GFP-treated BT-12 animals. The median survival for MV-GFP-treated BT-16 animals was 49 days ( $n = 13$ ; range: 35–89 days) compared with 30 days ( $n = 8$ ; range: 29–34 days) for UV-inactivated MV-GFP BT-16 animals.

Four out of 9 mice implanted with BT-12 and subsequently treated with MV-GFP survived to the experimental endpoint of 100 days (Fig. 3A). Upon pathological examination of their brains, there was no sign of viable tumor cells. However, there was evidence of the needle track in these animals, and it was typically associated with gliosis and hemosiderin-laden macrophages (data not shown). The remaining 5 BT-12 animals, along with the BT-16 MV-GFP-treated mice exhibited extensive areas of active MV infection (BT-12, (Fig. 4F); BT-16 (Fig. 4L). Conversely, the brains of animals treated with UV-inactivated MV-GFP contained large destructive tumors with mass effect (BT-12, Fig. 4A; BT-16, (Fig. 4G)).

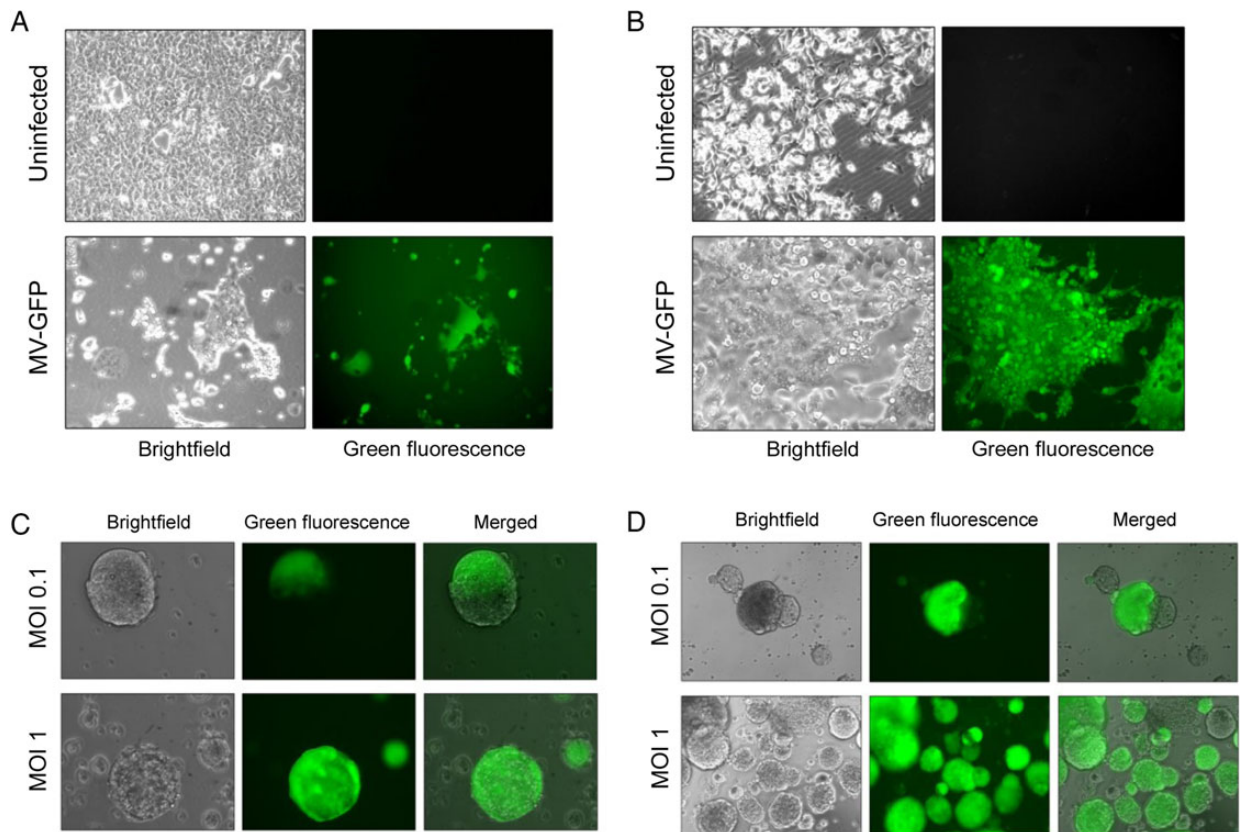


**Fig. 1.** Susceptibility of atypical teratoid rhabdoid tumor (AT/RT) cells to MV-GFP infection. The human AT/RT cell lines BT-16 (A) and BT-12 (B) infected with MV-GFP at a multiplicity of infection (MOI) of 0.1 showing GFP expression and syncytium formation 48 hours after infection. MV-GFP infection of neurospheres derived from BT-16 cells at 24 hours (C) and 48 hours (D) after infection.

### Measles Virus Increases Survival of Animals with Disseminated Atypical Teratoid Rhabdoid Tumor Disease

To determine the efficacy of MV treatment in our model of disseminated disease, we established AT/RT xenografts in athymic nude mice. Using stereotactic guidance, we injected BT-12 (Fig. 3B) and BT-16 (Fig. 3D) cells stably expressing firefly luciferase into the lateral ventricles of athymic nude mice, where the cells would have direct access to the cerebrospinal fluid. Animals were evaluated prior to MV treatment for a bioluminescent signal in the spinal cord, demonstrating disseminated disease (see Supplementary Fig. S1). Three days following tumor implantation, MV-GFP or UV-inactivated MV-GFP ( $5 \times 10^5$  pfu) was injected directly into the right lateral ventricle. The animals were then monitored to assess survival. There was a significant increase in survival of animals treated with MV-GFP compared with animals treated with UV-inactivated MV-GFP ( $P > .001$ , BT-12 [Fig. 3B];  $P < .001$ , BT-16 [Fig. 3D]). The median survival for MV-GFP-treated BT-12 tumors was 34 days ( $n = 9$ ; range: 27–45 days) compared with 15 days ( $n = 10$ ; range 14–17 days) for UV-inactivated MV-GFP-treated BT-12 animals. The median survival for MV-GFP-treated BT-16 tumors was 33.5 days ( $n = 10$ ; range: 28–83 days) compared with 14 days ( $n = 8$ ; range: 13–16 days) for UV-inactivated MV-GFP-treated BT-16 animals. There were no long-term survivors in the MV-GFP treatment group. Pathological review revealed

extensive intraventricular, intracranial subarachnoid, and spinal subarachnoid disease in both treated and untreated animals (BT-12, (Fig. 3B, D and F); BT-16, (Fig. 3H, J and K)).

### Intravenous Delivery of Measles Virus Increases Survival of Animals with Localized Atypical Teratoid Rhabdoid Tumor Disease

To assess the efficacy of intravenous delivery of MV, models of primary and disseminated disease were established for BT-12 and BT-16. As previously described, animals were treated with either MV-GFP or UV-inactivated MV-GFP ( $1 \times 10^6$  pfu/dose) for 7 or 3 days following tumor implantation for primary and disseminated disease, respectively. MV was delivered via the lateral tail vein. Unfortunately, MV treatment failed to significantly increase the survival of animals in any of the tumor or model systems evaluated (data not shown).

One of our limitations concerning MV therapy is the low titers achieved when manufacturing the virus. This, along with the volume we can safely deliver to a mouse via the tail vein, restricts the amount of virus we can deliver. To overcome this obstacle, we treated primary models of BT-12 and BT-16 at 7, 9, and 11 days following tumor implantation with either MV or UV-inactivated MV-GFP ( $1 \times 10^6$  pfu). MV treatment significantly increased the survival of both BT-12 ( $P = .0003$ ; Fig. 5A) and

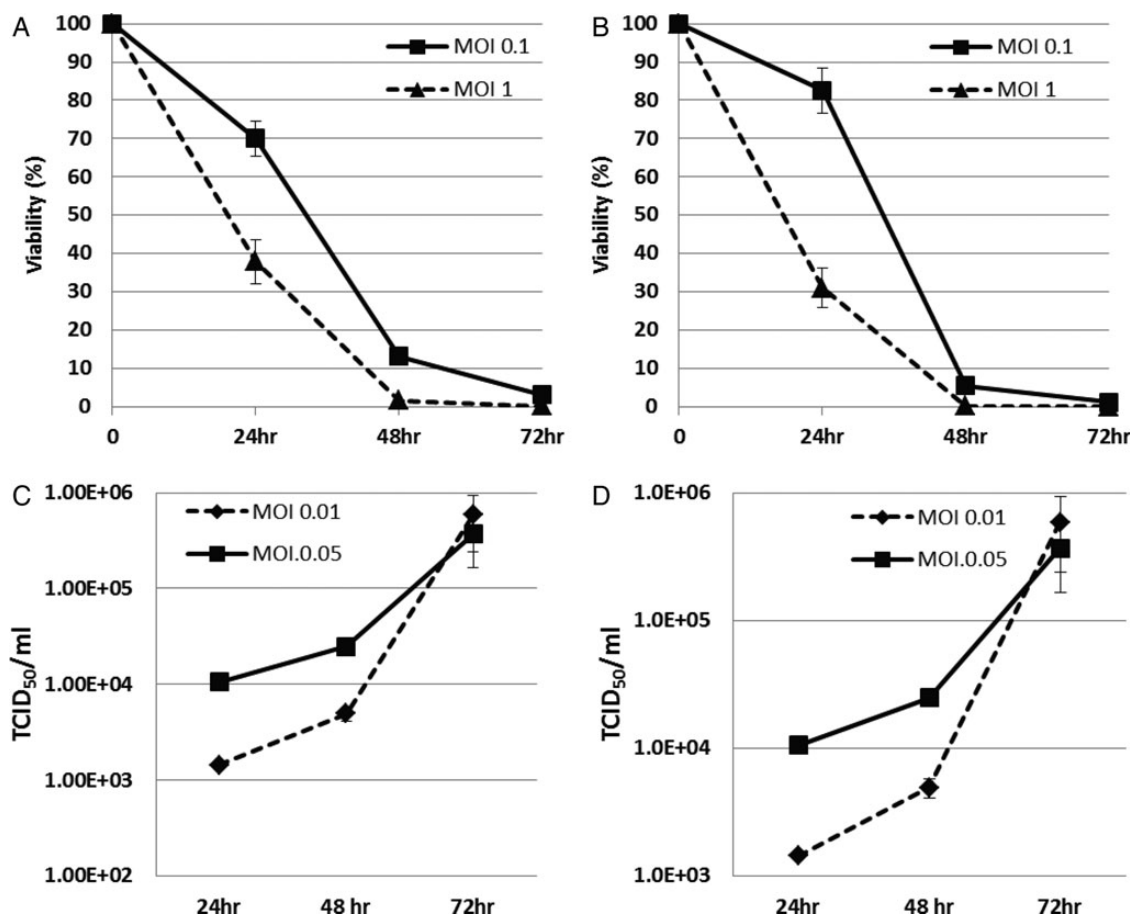


**Fig. 2.** Cytopathic effect and viral replication of MV-GFP in atypical teratoid rhabdoid tumor (AT/RT) cells. The viability of BT-12 (A) and BT-16 (B) human AT/RT cells following administration of MV-GFP at a multiplicity of infection (MOI) of 0.1 and 1. Less than 20% of the cells are viable at 48 hours after infection at an MOI of 0.1, and <1% of the cells are viable at 48 hours after infection at an MOI of 1. Replication of MV-GFP in BT-12 (A) and BT-16 (B) cells is demonstrated by the titers obtained at 24, 48 and 72 hours at an MOI of 0.01 and 0.05. Titration was done on Vero cells in a 96-well plate using the 50% end dilution method.

BT-16 ( $P < .0001$ ; Fig. 5B). The median survival for MV-GFP treated BT-12 animals was 49 days ( $n = 7$ ; range: 29–65 days) compared with 33 days ( $n = 12$ ; range: 30–37 days) for UV-inactivated MV-GFP-treated BT-12 animals. The median survival for MV-GFP-treated BT-16 animals was 65 days ( $n = 9$ ; range: 49–70 days) compared with 42 days ( $n = 9$ ; range: 34–51 days) for UV-inactivated MV-GFP BT-16 animals. A similar triple-dose MV treatment approach performed in the disseminated models once again failed to significantly increase survival.

IHC was performed on the brains and spinal cords of MV-treated animals 7 days after the last treatment to demonstrate MV dissemination and infection of tumor cells in the brain and spinal cord. Nucleoprotein immunoreactivity was detected in the cytoplasm of individual cells and multinucleated syncytia (Fig. 5C and D). MV infection of tumor cells located along the spinal cord was not detected in any of the animals evaluated ( $n = 5$ ).

## Discussion

An approach that is rapidly emerging as a potentially useful anticancer therapy is the use of oncolytic viruses. Numerous DNA and RNA viruses have demonstrated therapeutic efficacy

in preclinical studies leading to early phase clinical trials.<sup>14,16,26–33</sup> Within these clinical trials, acceptable safety and tolerance following virus administration has been observed in patients.<sup>14,16,28,34</sup> A successful oncolytic virus is one that selectively propagates and destroys cancerous tissue without causing excessive damage to the normal surrounding tissue.<sup>35</sup> Other groups have evaluated oncolytic viruses in the treatment of experimental animal models of AT/RT and demonstrated efficacy using recombinant vesicular stomatitis virus, myxoma virus, and vaccinia virus.<sup>36,37</sup> The purpose of this study was to determine if MV would be an effective therapeutic approach against preclinical models of AT/RT. The Edmonston's vaccine strain of MV has not only been administered safely to over a billion humans worldwide, it has proven to be an effective therapeutic agent against human tumors.<sup>10–13,21</sup> Furthermore, the safety of intracranial injection of MV has been previously demonstrated. Prior to initiating clinical trials for patients with glioblastoma, measles neurotoxicity studies were performed in previously immunized rhesus macaques, and no adverse effects were reported.<sup>15</sup>

Our study represents the first report that demonstrates efficacy of a recombinant MV in the treatment of AT/RT and the

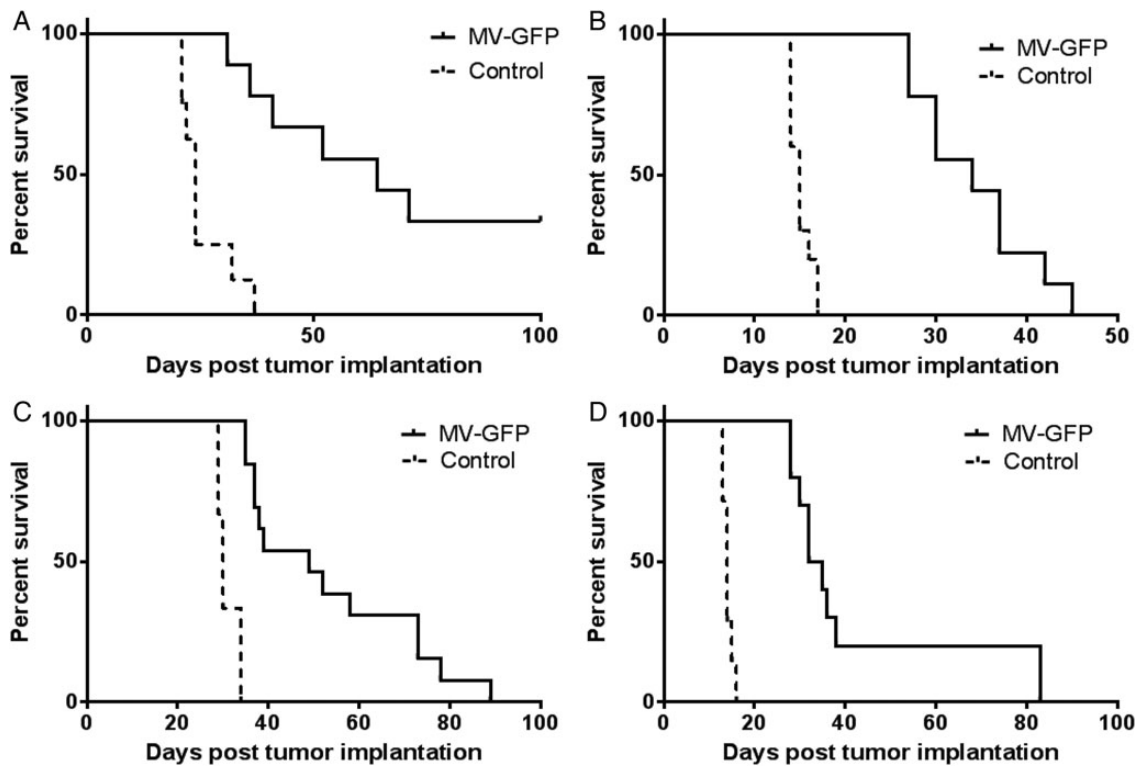


**Fig. 3.** Antitumor effect of MV-GFP. To model primary disease BT-12 (A) and BT-16 (C) Atypical teratoid rhabdoid tumors (AT/RTs) were established in the right frontal lobe of female athymic nude mice. Seven days after tumor implantation, the mice received a total of  $5 \times 10^5$  pfu of MV-GFP or the same dose of UV-inactivated MV-GFP. In both xenograft models, mice treated with MV-GFP had significantly longer survival than mice treated with UV-inactivated MV-GFP ( $P < .0001$ ). Four MV-GFP-treated animals implanted with BT-12 in the frontal lobe remained alive at the experimental endpoint (100 days). To model disseminated disease, BT-12 (B) and BT-16 (D) cells were injected into the right lateral ventricle of female athymic nude mice. Three days post tumor implantation the mice received a total of  $5 \times 10^5$  pfu of MV-GFP or the same dose of UV-MV-GFP injected directly into the right lateral ventricle. Mice treated with MV-GFP had significantly longer survival than mice treated with UV-MV-GFP ( $P < .0001$ ).

first study to report on the efficacy of an oncolytic virus for the treatment of disseminated AT/RT disease. The results from the study demonstrate significant antitumor activity of the modified MV against AT/RT cell lines in vitro. Cell killing was accompanied, as expected, by syncytia formation (Fig. 1). The cytotoxic effect was complete in 72 hours (Fig. 2A and B). Killing was seen at an MOI as low as 0.1, and essentially complete killing was seen at an MOI of 1.0. In addition, replication of the virus in the tumor cells was documented (Fig. 2C and D).

The data presented here also show that modified MV significantly prolongs survival of measles-treated animals in experimental models of primary and disseminated AT/RT disease (Fig. 3) when administered intratumorally. In the primary disease model of BT-12, 33% (3/9) of animals survived to the experimental endpoint. No viable tumor was detected upon pathological examination of the surviving animals. While none of the animals in the primary model of BT-12 or either of the disseminated models survived long term, we believe that the prolongation of survival is promising. Measles oncolytic virotherapy could be combined with current chemotherapies, which may allow a reduction in the chemotherapy dose for AT/RT, that could improve survival and/or limit the toxic long-term effect of chemotherapy in these young children.<sup>38-40</sup>

Intravenous administration of MV was performed to evaluate an alternative and potentially more clinically relevant

route of delivery. Initial studies administering one dose of MV failed to increase the survival of animals in either tumor model or disease model. However, a subsequent study treating animals every other day for a total of 3 treatments significantly increased the survival in BT-12 and BT-16 models of primary disease (Fig. 5). Multiple virus treatments did not increase the survival of the animals in the disseminated model cohorts. As has been previously demonstrated, the majority of MV administered intravenously is rapidly cleared from the blood stream, which provides an explanation for why the single virus injection failed to increase survival when the multiple injection protocol did.<sup>41</sup> Upon pathological examination of the brains in the single MV-treated study, cytopathic effect was observed in a subset of the animals, but it was minimal. The lack of a robust virus infection occurring in single-treated animals could potentially explain the failed survival increase. It is presumed that the multiple MV injections increased virus delivery to the tumor, leading to increased virus-induced cytopathic effect and ultimately increasing survival of the animals. Although we believe that multiple virus injections increased virus delivery to primary parenchymal tumors, we do not believe sufficient amounts of virus were able to reach sites of disseminated disease. As many of these sites of disseminated disease involve brain and spinal cord subarachnoid spaces, the amount of virus, even with repeated injections, may not have been sufficient to evade the

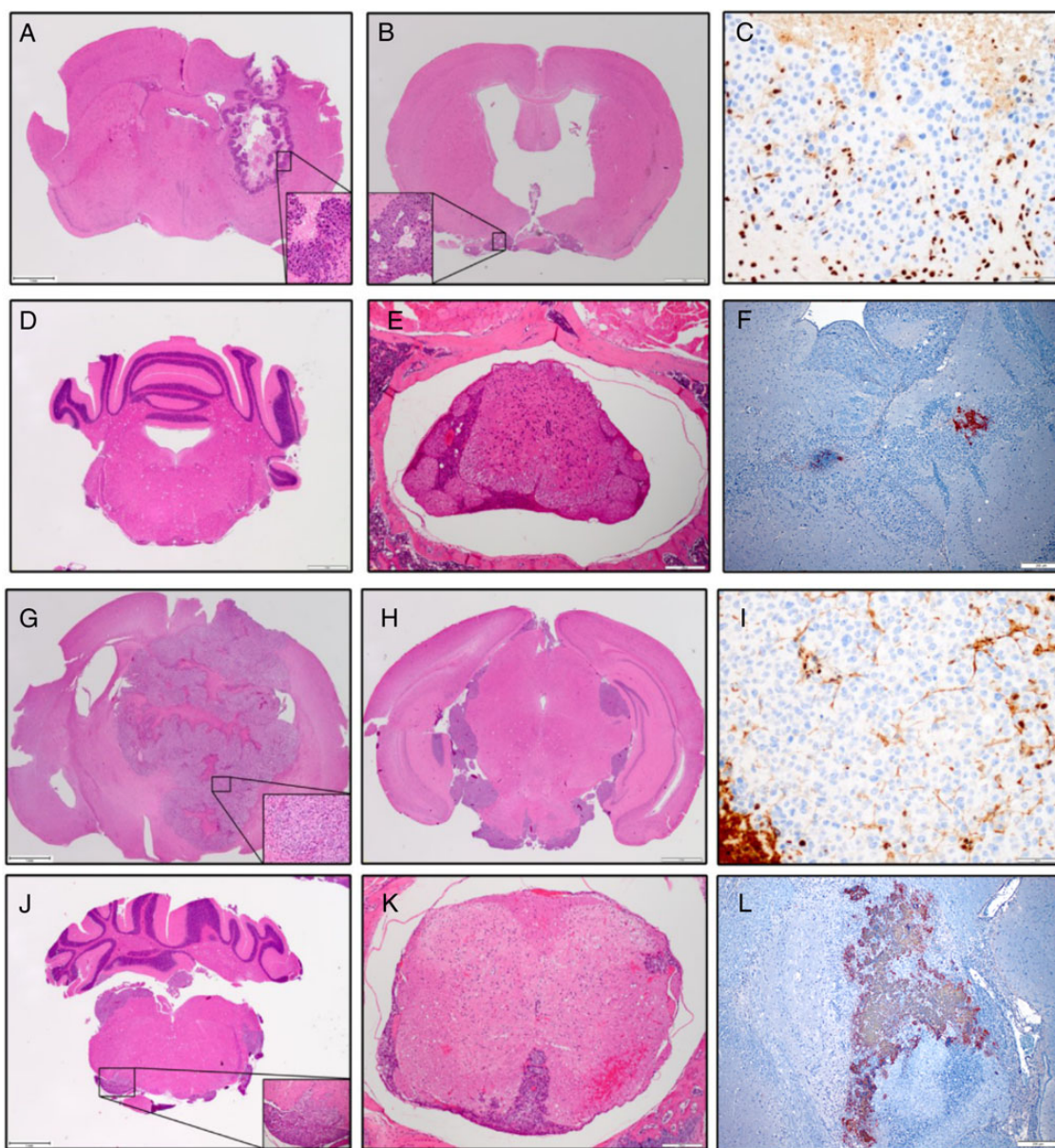


**Fig. 4.** Histological examination of mouse brains following injection of atypical teratoid rhabdoid tumor (AT/RT) cells and administration of MV-GFP. Primary and disseminated models of BT-12 (A–F) and BT-16 (G–L) disease were established in female athymic nude mice. AT/RT disease was observed in the primary tumor models of BT-12 (A) and BT-16 (G). Disseminated disease involving the subarachnoid space (B), intraventricular space (H), brainstem (D and J), and spinal cord (E and K) was observed. Paraffin-embedded tissue sections derived from BT-12 (C and F) and BT-16 (I and L) xenografts were stained with a mouse monoclonal anti-INI-1 antibody (C and I) and a rabbit polyclonal anti-MV nucleoprotein antibody (F and L). BT-12 (C) and BT-16 (I) derived xenografts failed to show INI-1 immunoreactivity. In comparison, mouse cells of the brain displayed INI-1 immunoreactivity. Measles-virus-treated BT-12 (F) and BT-16 (L) xenografts displayed measles nucleoprotein immunoreactivity in the cytoplasm of individual cells and multinucleated syncytia. Hematoxylin & eosin micrographs (x20); immunohistochemical micrographs (x100).

reticuloendothelial system, cross the blood-brain barrier, and access the cerebrospinal fluid to reach distant sites of disseminated disease. Future studies evaluating increased viral injections or mechanisms to increase serum bioavailability may lead to increased delivery to distant disseminated sites and enhanced survival.

As alluded to above, systemic delivery of MV poses numerous challenges in an immunized patient population. While it is

difficult to investigate these challenges in immune-compromised preclinical models, numerous recent studies have reported on strategies to improve delivery. Iankov et al reported efficacy in a multiple myeloma xenograft model in the presence of anti-measles antibodies using infected cell carriers (irradiated myeloma cells) to deliver MV to tumor cells.<sup>42</sup> Additional carriers including dendritic cells, mesenchymal stem cells, and bone marrow-derived mesenchymal stromal cells have all been

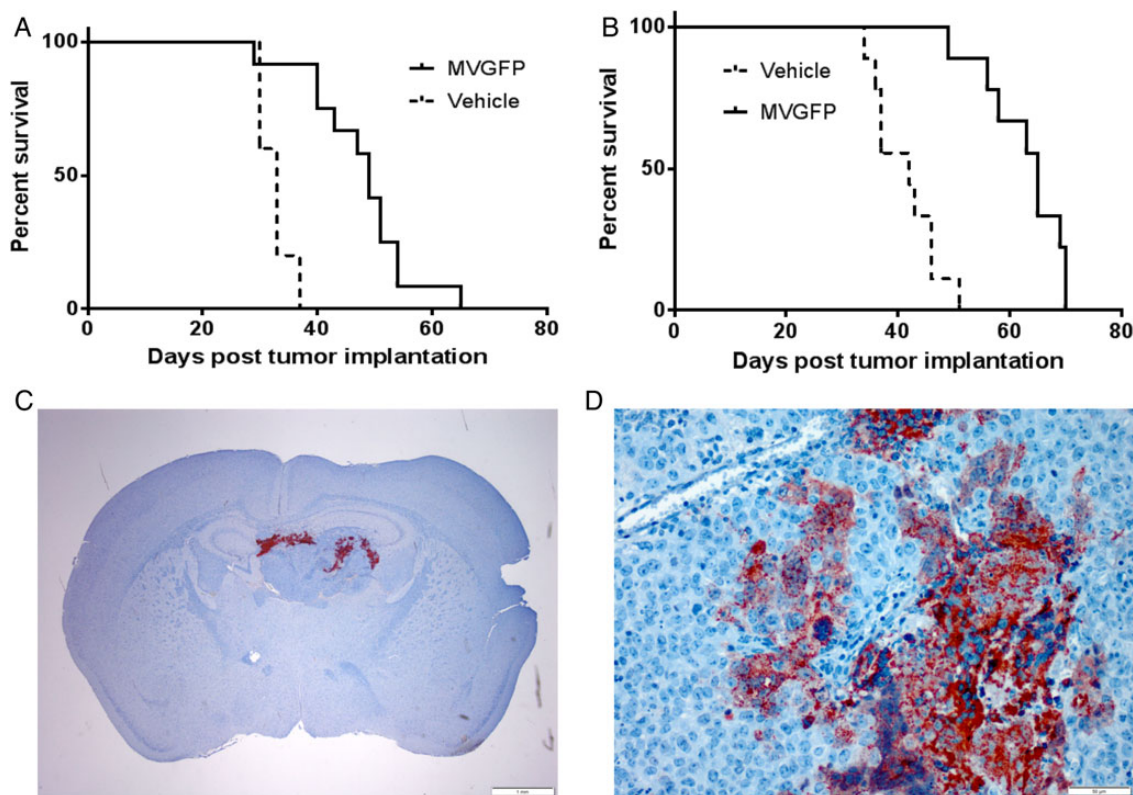


**Fig. 5.** Antitumor effect following intravenous delivery of MV-GFP. BT-12 (A) and BT-16 (B) primary tumors were established in the right frontal lobes of female athymic nude mice. Mice were treated with  $1 \times 10^6$  pfu MV-GFP or the same dose of UV MV-GFP at 7, 9, and 11 days post tumor implantation. MV-GFP or UV MV-GFP was delivered via the lateral tail vein. Mice treated with MV-GFP had significantly longer survival than mice treated with UV-MV-GFP (BT-12,  $P = .0003$ ; BT-16,  $P < .0001$ ). Paraffin-embedded tissue sections derived from BT-12 xenografts were stained with a rabbit polyclonal MV nucleoprotein antibody. Nucleoprotein immunoreactivity was detected in the cytoplasm of individual cells and multinucleated syncytia (C,  $\times 20$ ; D,  $\times 400$ ).

used to deliver MV in immune-competent xenograft models.<sup>11,43,44</sup> While, understanding and augmenting systemic delivery of MV to tumor is important, we believe intratumoral delivery is the most logical and effective delivery method. Systemic delivery is the optimal approach to target metastatic disease; however, systemic metastasis is very infrequent in AT/RT, and disseminated spread is within the CNS. Furthermore, the blood-brain-barrier provides an additional obstacle for delivery of MV to the brain.

While large-scale immunization campaigns have proven the safety of vaccine strains of MVs, preexisting antiviral immunity due to immunization and evidence of direct activation of the immune system in immune-competent preclinical models underscore the potential role of the immune system in developing an efficacious measles virotherapy platform.<sup>45-47</sup> Traditionally, it was believed that the host antiviral immune response would compromise oncolytic therapies. Rapid clearance of the virus would take place shortly after introduction in immunized hosts. A recent human trial evaluating intravenous delivery of MV to treat drug-refractory multiple myeloma supports this belief.<sup>16</sup> In that study 2 out of the 4 participants receiving the highest dose of virus responded to therapy. Both responders lacked detectable neutralizing anti-measles antibody.

In the setting of brain tumors, however, patients are often immunosuppressed due to the chemotherapeutic drugs

(eg, temozolomide, methotrexate, and cyclophosphamide) they receive.<sup>48</sup> Furthermore, most tumors, including brain tumors, express cytokines such as TGF- $\beta$  and recruit T-regulatory cells that help maintain an immunosuppressive microenvironment.<sup>49</sup> Unfortunately, at this time there are no immune-competent preclinical models of AT/RT to evaluate the influence of the immune system on tumor clearance. Such a model would be ideal to parse out the antitumor effect attributed to the oncolytic virus and the antitumor effect associated with the immune system.

In summary, our results demonstrate that a modified MV can infect and replicate in human AT/RT cell lines and exhibit significant therapeutic effect in intracranial and disseminated tumors. MV could provide a new therapeutic option for treating patients with AT/RT, especially those patients who fail or are ineligible for existing multimodality therapy. The encouraging results from this study, combined with the promising clinical results in other tumor types, suggest that this approach has therapeutic potential, and further studies are warranted to develop MV as a future treatment approach for AT/RT.

### Supplementary material

Supplementary material is available online at *Neuro-Oncology* (<http://neuro-oncology.oxfordjournals.org/>).



## Funding

Studies performed in the preceding manuscript were funded by a Nationwide Children's Hospital start-up grant awarded to E.M.J. This work was also supported by a CancerFree KIDS Pediatric Cancer Research Alliance award to A.W.S.

**Conflict of interest statement.** The authors declare no conflict of interest.

## References

- Biegel JA, Zhou JY, Rorke LB, et al. Germ-line and acquired mutations of INI1 in atypical teratoid and rhabdoid tumors. *Cancer Res.* 1999;59(1):74–79.
- Biegel JA, Tan L, Zhang F, et al. Alterations of the hSNF5/INI1 gene in central nervous system atypical teratoid/rhabdoid tumors and renal and extrarenal rhabdoid tumors. *Clin Cancer Res.* 2002; 8(11):3461–3467.
- Versteeg I, Sevenet N, Lange J, et al. Truncating mutations of hSNF5/INI1 in aggressive paediatric cancer. *Nature.* 1998; 394(6689):203–206.
- Bhattacharjee M, Hicks J, Langford L, et al. Central nervous system atypical teratoid/rhabdoid tumors of infancy and childhood. *Ultrastruct Pathol.* 1997;21(4):369–378.
- Parwani AV, Stelow EB, Pambuccian SE, et al. Atypical teratoid/rhabdoid tumor of the brain: cytopathologic characteristics and differential diagnosis. *Cancer.* 2005;105(2):65–70.
- Jackson EM, Sievert AJ, Gai X, et al. Genomic analysis using high-density single nucleotide polymorphism-based oligonucleotide arrays and multiplex ligation-dependent probe amplification provides a comprehensive analysis of INI1/SMARCB1 in malignant rhabdoid tumors. *Clin Cancer Res.* 2009;15(6): 1923–1930.
- Biegel JA. Molecular genetics of atypical teratoid/rhabdoid tumor. *Neurosurg Focus.* 2006;20(1):E11–E10.
- Russell SJ, Peng KW. Viruses as anticancer drugs. *Trends Pharmacol Sci.* 2007;28(7):326–333.
- Parato KA, Senger D, Forsyth PA, et al. Recent progress in the battle between oncolytic viruses and tumours. *Nat Rev Cancer.* 2005; 5(12):965–976.
- Allen C, Paraskevovou G, Liu C, et al. Oncolytic measles virus strains in the treatment of gliomas. *Expert Opin Biol Ther.* 2008; 8(2):213–220.
- Iankov ID, Msaouel P, Allen C, et al. Demonstration of anti-tumor activity of oncolytic measles virus strains in a malignant pleural effusion breast cancer model. *Breast Cancer Res Treat.* 2010; 122(3):745–754.
- Liu C, Sarkaria JN, Petell CA, et al. Combination of measles virus virotherapy and radiation therapy has synergistic activity in the treatment of glioblastoma multiforme. *Clin Cancer Res.* 2007; 13(23):7155–7165.
- Msaouel P, Iankov ID, Allen C, et al. Engineered measles virus as a novel oncolytic therapy against prostate cancer. *Prostate.* 2009; 69(1):82–91.
- Galanis E, Hartmann LC, Cliby WA, et al. Phase I trial of intraperitoneal administration of an oncolytic measles virus strain engineered to express carcinoembryonic antigen for recurrent ovarian cancer. *Cancer Res.* 2010;70(3):875–882.
- Myers R, Harvey M, Kaufmann TJ, et al. Toxicology study of repeat intracerebral administration of a measles virus derivative producing carcinoembryonic antigen in rhesus macaques in support of a phase I/II clinical trial for patients with recurrent gliomas. *Hum Gene Ther.* 2008;19(7):690–698.
- Russell SJ, Federspiel MJ, Peng KW, et al. Remission of disseminated cancer after systemic oncolytic virotherapy. *Mayo Clin Proc.* 2014;89(7):926–933.
- Dhiman N, Jacobson RM, Poland GA. Measles virus receptors: SLAM and CD46. *Rev Med Virol.* 2004;14(4):217–229.
- Russell SJ, Peng KW. Measles virus for cancer therapy. *Curr Top Microbiol Immunol.* 2009;330:213–241.
- Grote D, Russell SJ, Cornu TI, et al. Live attenuated measles virus induces regression of human lymphoma xenografts in immunodeficient mice. *Blood.* 2001;97(12):3746–3754.
- Peng KW, TenEyck CJ, Galanis E, et al. Intraperitoneal therapy of ovarian cancer using an engineered measles virus. *Cancer Res.* 2002;62(16):4656–4662.
- Studebaker AW, Kreofsky CR, Pierson CR, et al. Treatment of medulloblastoma with a modified measles virus. *Neuro Oncol.* 2010;12(10):1034–1042.
- Studebaker AW, Hutzen B, Pierson CR, et al. Oncolytic measles virus prolongs survival in a murine model of cerebral spinal fluid-disseminated medulloblastoma. *Neuro Oncol.* 2012;14(4): 459–470.
- D'Conja J, Shalaby T, Rivera P, et al. Antisense treatment of IGF-IR induces apoptosis and enhances chemosensitivity in central nervous system atypical teratoid/rhabdoid tumours cells. *Eur J Cancer.* 2007;43(10):1581–1589.
- Phuong LK, Allen C, Peng KW, et al. Use of a vaccine strain of measles virus genetically engineered to produce carcinoembryonic antigen as a novel therapeutic agent against glioblastoma multiforme. *Cancer Res.* 2003;63(10):2462–2469.
- Hemmati HD, Nakano I, Lazareff JA, et al. Cancerous stem cells can arise from pediatric brain tumors. *Proc Natl Acad Sci USA.* 2003;100(25):15178–15183.
- Bourke MG, Salwa S, Harrington KJ, et al. The emerging role of viruses in the treatment of solid tumours. *Cancer Treat Rev.* 2011;37(8):618–632.
- Donnelly O, Harrington K, Melcher A, et al. Live viruses to treat cancer. *J R Soc Med.* 2013;106(8):310–314.
- Donnelly OG, Errington-Mais F, Prestwich R, et al. Recent clinical experience with oncolytic viruses. *Curr Pharm Biotechnol.* 2012; 13(9):1834–1841.
- Eager RM, Nemunaitis J. Clinical development directions in oncolytic viral therapy. *Cancer Gene Ther.* 2011;18(5):305–317.
- Miest TS, Cattaneo R. New viruses for cancer therapy: meeting clinical needs. *Nat Rev Microbiol.* 2014;12(1):23–34.
- Patel MR, Kratzke RA. Oncolytic virus therapy for cancer: the first wave of translational clinical trials. *Transl Res.* 2013;161(4): 355–364.
- Russell SJ, Peng KW, Bell JC. Oncolytic virotherapy. *Nat Biotechnol.* 2012;30(7):658–670.
- Vacchelli E, Eggermont A, Sautes-Fridman C, et al. Trial watch: Oncolytic viruses for cancer therapy. *Oncoimmunology.* 2013; 2(6):e24612.
- Hammill AM, Conner J, Cripe TP. Oncolytic virotherapy reaches adolescence. *Pediatr Blood Cancer.* 2010;55(7):1253–1263.

35. Galanis E. Therapeutic potential of oncolytic measles virus: promises and challenges. *Clin Pharmacol Ther.* 2010;88(5):620–625.
36. Wu Y, Lun X, Zhou H, et al. Oncolytic efficacy of recombinant vesicular stomatitis virus and myxoma virus in experimental models of rhabdoid tumors. *Clin Cancer Res.* 2008;14(4):1218–1227.
37. Lun X, Ruan Y, Jayanthan A, et al. Double-deleted vaccinia virus in virotherapy for refractory and metastatic pediatric solid tumors. *Mol Oncol.* 2013;7(5):944–954.
38. Gardner SL, Asgharzadeh S, Green A, et al. Intensive induction chemotherapy followed by high dose chemotherapy with autologous hematopoietic progenitor cell rescue in young children newly diagnosed with central nervous system atypical teratoid rhabdoid tumors. *Pediatr Blood Cancer.* 2008;51(2):235–240.
39. Chi SN, Zimmerman MA, Yao X, et al. Intensive multimodality treatment for children with newly diagnosed CNS atypical teratoid rhabdoid tumor. *J Clin Oncol.* 2009;27(3):385–389.
40. Zaky W, Dhall G, Ji L, et al. Intensive induction chemotherapy followed by myeloablative chemotherapy with autologous hematopoietic progenitor cell rescue for young children newly-diagnosed with central nervous system atypical teratoid/rhabdoid tumors: the Head Start III experience. *Pediatr Blood Cancer.* 2014;61(1):95–101.
41. Liu YP, Tong C, Dispenzieri A, et al. Polyinosinic acid decreases sequestration and improves systemic therapy of measles virus. *Cancer Gene Ther.* 2012;19(3):202–211.
42. Iankov ID, Blechacz B, Liu C, et al. Infected cell carriers: a new strategy for systemic delivery of oncolytic measles viruses in cancer virotherapy. *Mol Ther.* 2007;15(1):114–122.
43. Mader EK, Maeyama Y, Lin Y, et al. Mesenchymal stem cell carriers protect oncolytic measles viruses from antibody neutralization in an orthotopic ovarian cancer therapy model. *Clin Cancer Res.* 2009;15(23):7246–7255.
44. Castleton A, Dey A, Beaton B, et al. Human mesenchymal stromal cells deliver systemic oncolytic measles virus to treat acute lymphoblastic leukemia in the presence of humoral immunity. *Blood.* 2014;123(9):1327–1335.
45. Kumar H, Kawai T, Akira S. Toll-like receptors and innate immunity. *Biochem Biophys Res Commun.* 2009;388(4):621–625.
46. Gilliet M, Cao W, Liu YJ. Plasmacytoid dendritic cells: sensing nucleic acids in viral infection and autoimmune diseases. *Nat Rev Immunol.* 2008;8(8):594–606.
47. Guillerme JB, Boisgerault N, Roulois D, et al. Measles virus vaccine-infected tumor cells induce tumor antigen cross-presentation by human plasmacytoid dendritic cells. *Clin Cancer Res.* 2013;19(5):1147–1158.
48. Stepkowski SM. Molecular targets for existing and novel immunosuppressive drugs. *Expert Rev Mol Med.* 2000;2(4):1–23.
49. Vandenberk L, Van Gool SW. Treg infiltration in glioma: a hurdle for antiglioma immunotherapy. *Immunotherapy.* 2012;4(7):675–678.